THE ENERGY DEPENDENCE OF THE $\vec{(p,d)}$ REACTION FOR ^{54}Fe AND ^{140}Ce

S.A. Dickey, J.J. Kraushaar, and J.R. Shepard
University of Colorado, Boulder, Colorado 80309

D.W. Miller, C.W. Glover, and W.P. Jones
Indiana University Cyclotron Facility, Bloomington, Indiana 47405

The data acquired at 122 MeV for the ^{54}Fe(p,d) and ^{140}Ce(p,d) reactions have now been completely analyzed and cross sections and analyzing powers for all of the observed transitions are available. The cross sections for the ^{54}Fe data are shown in Fig. 1 and analyzing powers are shown in Fig. 2. Figs. 3 and 4 show the corresponding data for ^{140}Ce.

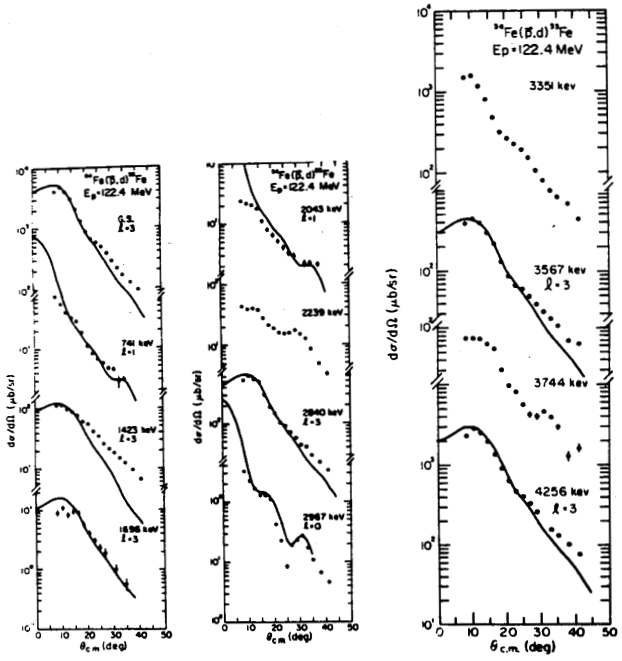

Figure 1. Angular distributions for the ^{54}Fe$\vec{(p,d)}^{53}$Fe reaction at 122 MeV. The curves shown are the results of exact finite-range calculations for the ℓ-values listed in Table I using an adiabatic deuteron optical model potential.

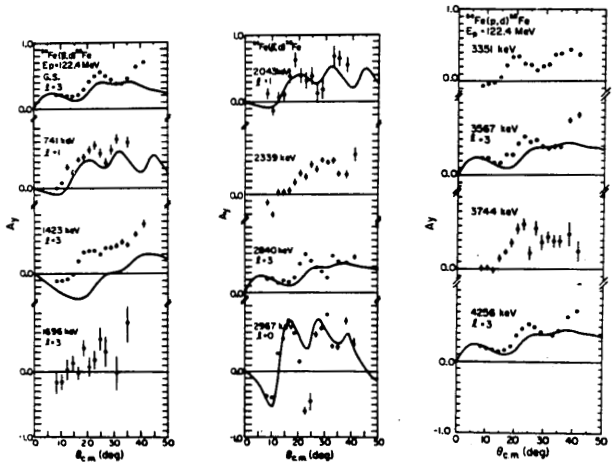

Figure 2. Analyzing powers for the ^{54}Fe$\vec{(p,d)}^{53}$Fe reaction at 122 MeV. The curves shown are the results of exact finite-range calculations.

The primary purpose of these studies was to examine the energy dependence of the (p,d) reaction on some nuclei with closed neutron shells to see if the trends observed[1] for ^{208}Pb are more general. In ^{208}Pb it was noted that the spectroscopic factors for high ℓ-values, in particular, tend to decrease dramatically at energies above about 50 MeV.

Data are available on ^{54}Fe and ^{140}Ce at several lower energies and these data along with the present data at 122 MeV were compared with distorted wave calculations in order to extract spectroscopic factors.

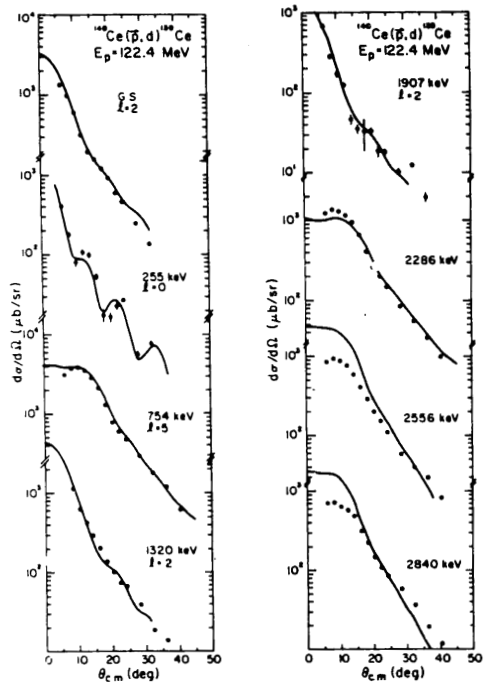

Figure 3. Angular distributions for the ^{140}Ce(p,d)^{139}Ce reaction at 122 MeV. The curves shown are the results of exact finite-range calculations to the ℓ-values listed in Table I, using an adiabatic deuteron optical model potential.

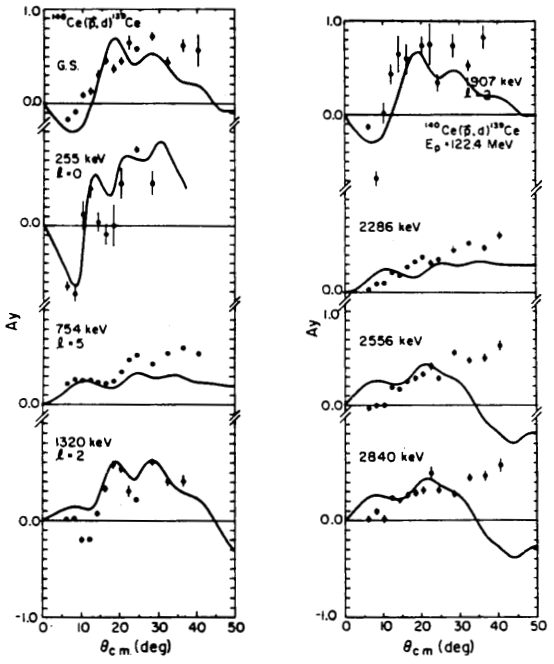

Figure 4. Analyzing powers for the ^{140}Ce($\vec{p}$,d)^{139}Ce reaction at 122 MeV. The curves shown are the results of exact finite-range calculations utilizing an adiabatic deuteron optical model potential.

The calculations were carried out using the exact finite-range DWBA program DWUCK-5. The proton optical model potentials were taken from references 2 and 3. Adiabatic deuteron potentials were constructed from proton parameters from the same sources. Non-locality correction factors of 0.85 and 0.54 for the proton and deuteron, respectively, were used. The bound state radius parameter was set at 1.25 fm and the diffuseness at 0.65 fm. The results of these calculations are shown as the solid lines in Figs. 1 through 4. The analyzing power data are described suprisingly well by the calculations.

Spectroscopic factors were extracted from the 122 MeV data and the lower energy data for both nuclei and the results are presented in Table I. As in the case of ^{208}Pb, the spectroscopic factors for the ^{54}Fe and ^{140}Ce data for the higher ℓ-values tended to decrease as the incident projectile energy increases. This behavior of the spectroscopic factors further emphasizes the need to reexamine the reaction mechanism as it is used in the current DWBA theory. Possible solutions may emerge from work involving relativistic Dirac calculations. This research, however, is still in the beginning stages and its application to transfer reactions, or specifically, the (p,d) reaction, is not yet available.

Further analysis of the data will continue. There are some calculations which are now being carried out which can better handle the continuum states of the deuterons. This, combined with work being done to determine better non-locality parameters to be used at the higher energies, may yield a better description of the cross section and analyzing power data.

TABLE I

Spectroscopic Factors as a Function of Incident Proton Energy for ^{53}Fe and ^{139}Ce

^{54}Fe (p,d) ^{53}Fe						^{140}Ce (p,d) ^{139}Ce				
		$C^2S\ell_j$						$C^2S\ell_j$		
Excitation Energy (keV)	ℓ-Value	a) 29 MeV	b) 40 MeV	c) 52 MeV	122 MeV	Excitation Energy (keV)	ℓ-value	d) 24.6 MeV	e) 35 MeV	122 MeV
0.0	3	4.6	3.48	3.0	1.9	0.0	2	4.0	4.6	1.92
741	1	0.048	0.05	0.06	0.099	255	0	1.6	1.6	1.5
1423	3	0.052	0.08	(0.07)	0.07	754	5	9.1	8.1	1.62
2043	1	0.05	0.06	0.04	0.047	1320	2	1.76	3.0	3.3
2840	3	0.47	0.39	0.31	0.22	1907	J=5/2	0.8	1.2	0.83
							J=7/2			0.55
2967	0	---	1.31	1.2	1.1	2286	5	---	2.0	0.43

a) ref. 4
b) ref. 5
c) ref. 6
d) ref. 7
e) ref. 8

1) S.A. Dickey, J.J. Kraushaar and M.A. Rumore, Nucl. Phys. A391, 413 (1982).

2) F.D. Becchetti, Jr. and G.W. Greenless, Phys. Rev. 182, 1190 (1969).

3) P. Schwandt et al., Phys. Rev. C 26, 55 (1982).

4) R.O. Nelson et al., Nucl. Phys. A215, 541 (1973).

5) T. Suehiro et al., Nucl. Phys. A313, 141 (1979).

6) H. Ohnuma et al., J. Phys. Soc. Japan 32, 1466 (1972).

7) A. Chaumeaux, G. Bruge, H. Faraggi and J. Picard, Nucl. Phys. A164, 176 (1971).

8) R.K. Jolly and E. Kashy, Phys. Rev. C 4, 1398 (1971).